Optica Applicata, Vol. XIX, No. 3, 1989

Influence of aberrations on the imaging of short light pulses by holographic concave gratings

R. GÜTHER

Central Institute for Optics and Spectroscopy of the Academy of Sciences of the GDR, 1199 Berlin-Adlershof, Rudower Chaussee 6, GDR.

We treat the influence of a corrected holographic concave grating on the image of a short light pulse, using a time-dependent ray tracing and a time-dependent diffraction theory. The pulse is lengthened by a duration the light needs for scanning the grating. This lengthened pulse can be split into multiple pulses by aberrations.

1. Introduction

In short-time spectroscopy [1] high luminosity corrected holographic concave gratings ($f/3$) and pulses of a few ten picoseconds are used. Then, however, the light pulse does not cover completely the surface of the diffraction grating during its propagation from the source A to the receiver B (see Fig. 1)

General considerations on the connection between spatial structures and time behaviour were made by VIENOT et al. [2] in the framework of "four-dimensional optics". A similar treatment using the correlation function was given in [3], [4]; its special purpose was spectral analysis of short pulses made by instruments without aberrations. The time response caused by grating aberrations was first considered in [5]. The difference between the phase front and the pulse front in lens systems and Fresnel zone plates was treated in [6]. In such systems the possibilities of the pulse front deformation correction are connected with the achromatic correction of the optical system.

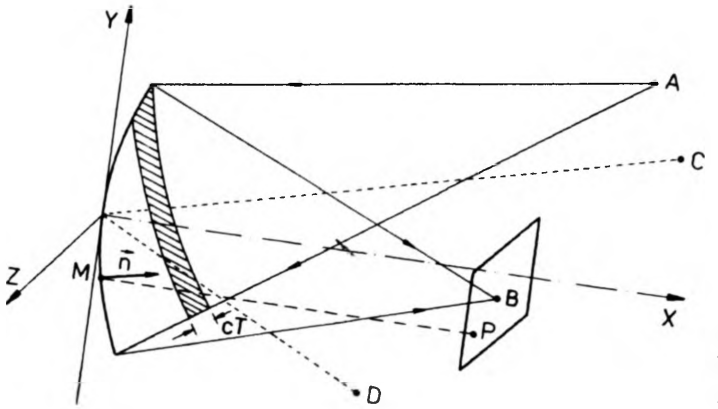

Fig. 1. Diffraction of a short light pulse by a corrected holographic concave grating

Here, we treat the influence of aberrations on the time-dependent imaging by corrected holographic concave gratings. The aberrations can be considerable if the tuning of a single grating monochromator ranges, for instance, within 500 nm ([7], [8]). The calculation methods are based on a time-dependent diffraction theory and a time-dependent ray tracing. We treat solely the unchirped pulses and assume constant diffraction amplitudes of the fields. The effects considered here are essential for the pulse duration ranging between 10 ps and 100 ps. The compensation of the pulse propagation time for the range of a few picoseconds in double monochromators composed of holographic gratings will be treated in a forthcoming paper.

2. Time-dependent diffraction

The formulae for time-dependent diffraction are ([9], [10]):

$$V(P,t) = \frac{1}{4\pi}\iint_S \left\{[V]\frac{\partial}{\partial n}\left(\frac{1}{s}\right) - \frac{1}{cs}\frac{\partial s}{\partial n}\left[\frac{\partial V}{\partial t}\right] - \frac{1}{s}\left[\frac{\partial V}{\partial n}\right]\right\} dS_M, \tag{1}$$

$$= \frac{1}{4\pi}\iint_S dS_M \frac{1}{\sqrt{2\pi}}\int_{-\infty}^{+\infty}\left\langle U_\omega\left\{\frac{\partial}{\partial n}\left(\frac{1}{s}\right) + \frac{i\omega}{cs}\frac{\partial s}{\partial n}\right\} e^{-i\omega(t-s/c)} - \frac{e^{-i\omega(t-s/c)}}{s}\frac{\partial U_\omega}{\partial n}\right\rangle d\omega \tag{2}$$

with

$$U_\omega(x,y,z) = \frac{1}{\sqrt{2\pi}}\int_{-\infty}^{+\infty} V(x,y,z,t)\, e^{i\omega t}\, dt.$$

Both formulations are useful for the discussion of the approximations to be performed. In these formulae: V is the field with all the time dependence; U_ω – the temporal Fourier transform; s – the distance between point M on the grating surface S and image point P; c – the velocity of light, and $\partial/\partial n$ is the normal derivation with reference to the grating surface; [...] means that after the calculation of the internal term the retarded time $(t - s/c)$ should be used.

In the first approximation step we find in (2) $\left|\frac{\partial}{\partial n}\left(\frac{1}{s}\right)\right| \ll \left|\frac{i\omega}{cs}\frac{\partial s}{\partial n}\right|$, because every derivation made with $s = \overline{MP}$ is small compared to ω/c by a factor $10^5 \ldots 10^6$.

In Equation (1) we multiply the integrand by the factor

$$\exp\left\{i\frac{2\pi}{\lambda_0}(\overline{CM} - \overline{DM})\frac{\hat{k}\lambda_0}{\hat{\lambda}}\right\},$$

which means the phase change caused by point M moving from groove to groove on the grating surface S. In the holography this is the phase function generated by the interference pattern of the object wave and the reference wave. Here, the holographic grating is produced by the interference of the spherical waves which start from the point sources C and D [11]. Therefore, the distances $\overline{CM}$ and $\overline{DM}$ between the point sources C and D and point M (Fig. 1) generate the phase difference. $\hat{k}$ is the order of

diffraction, $\hat{\lambda}$ – the wavelength of light used for production of the grating, and λ_0 – the wavelength of the grating used.

The incident field is the product of a slowly varying amplitude and the phase (Fig. 1)

$$V(M,t) = U(k_0\overline{MA} - \omega t)\exp\{ik_0\overline{MA} - i\omega_0 t\}/\overline{MA}. \tag{3}$$

We obtain

$$V(P,t) = \frac{1}{4\pi}\iint_S dS_M \left\{ -\frac{1}{c\,\overline{MP}}\frac{\partial\overline{MP}}{\partial n}\left[\frac{\partial}{\partial t}\left\langle U(k_0\overline{MA} - \omega_0 t) \times \exp(ik_0\overline{MA} - i\omega_0 t)/\overline{MA}\right\rangle\right] - \frac{1}{\overline{MP}}\left[\frac{\partial}{\partial n}\left\langle U(k_0\overline{MA} - \omega_0 t) \times \exp(ik_0\overline{MA} - i\omega_0 t)/\overline{MA}\right\rangle\right]\right\} \exp i\left[\frac{2\pi}{\lambda_0}(\overline{CM} - \overline{DM})\frac{\hat{k}\lambda_0}{\hat{\lambda}}\right], \tag{4}$$

k_0 is given by $2\pi/\lambda_0$. We emphasize the convention on the brackets [...] given in connection with Eq. (1). The position of the surface element dS_M varies with M. Finally, the sign of the local cos $(\vec{n}, \vec{MA})$ is inverted because of reflection. We suppose:

$$\left|\frac{\frac{\partial\overline{MA}}{\partial n}}{\overline{MA}}\right| \ll \left|ik_0\frac{MA}{b}\right|, \qquad |\cos(\vec{MP}, \vec{n})| + |\cos(\vec{MA}, \vec{n})| \approx 2$$

and

$$\frac{1}{\overline{MA}\,\overline{MP}} \approx \text{const.}$$

After all differentiations we get the equation

$$V(P,t) = \text{const}\, e^{-i\omega_0 t}\iint_S (iU(\tau) + U'(\tau)) \times \exp\left\{ik_0\left[\overline{MA} + \overline{MP} - \frac{\hat{k}\lambda_0}{\hat{\lambda}}(\overline{CM} - \overline{DM})\right]\right\} dS_M \tag{5}$$

where $\tau = k_0[\overline{MA} + \overline{MP}] - \omega_0(t - t_0)$. The addition of t_0 means a possible translation of the zero point of the time which is useful in the practical calculations. In Equation (5) the orders of magnitude are for our purposes $|U(\tau)| \approx (10^4 \ldots 10^5)|U'(\tau)|$. This offers a further approximation down to the "quasi-stationary" use of $U(\tau)$ only. A pulse shape of $U(\tau)$ causes an actual integration on a limited part of the grating surface as shown in Fig. 1. Equation (5) was programmed on a desk-top computer. P varies in a plane perpendicularly to the central ray $\overline{MB}$. In the case of one-dimensional simplifications (Y-integration only), we multiply sometimes the integrand of Eq. (5) by an additional phase factor $\exp\{ik_0(DY^2 + K_1Y^3 + SY^4)\}$ in order to consider the effects of defocusing D, meridional coma K_1, or spherical aberration S. These aberrations occur in the light path function of the grating theory ([7], [11]).

3. Time-dependent ray tracing

Large phases in Equation (5) produce high frequency oscillations of the integrand, giving rise to errors in the numerical integration. Therefore, we look for the results of purely geometrical ray tracing. The usual ray tracing procedure for gratings [7] is being combined with the demand that a spot in the spot diagram be plotted only if the optical path length and detection time fit the pulse length

$$\overline{AM} + \overline{MP} - c(t - t_0) = \pm cT/2, \tag{6}$$

where T is the pulse lenght of a rectangular pulse. Given pulse shapes could be modelled by counting the "fractions of spots" per area, but we intend to study the principal effects. The condition (6) cuts out a range of points M on the grating surface with the limits

$$\overline{AM} + \overline{MP} - c(t - t_0) = \pm cT/2$$

time t being given. This range has a characteristic width w on the grating resulting in a characteristic diffraction width w' in the focal plane. Finally, we keep w' smaller than the effects we have found by ray tracing.

4. Images by diffraction

Firstly, we consider the ideal stigmatic focusing which may be achieved by the use of a corrected holographic concave grating type III [11] of the following production parameters $\hat{\lambda} = 458$ nm, $l_C = 28.284$ cm, $\gamma = 45°$ (polar coordinates of point C), $l_D = 20$ cm, $\delta = 0°$ (polar coordinates of point D), $R = 20$ cm (radius of curvature of the grating support), and the parameters used: $\lambda_0 = 458$ nm, $l_A = 28.284$ cm, $\alpha = 45°$ (polar coordinates of the slit), grating extension in the Y-Z plane -2 cm $< Y, Z < 2$ cm. We assume for $U(\tau)$ a Gaussian pulse with the temporal width $T = 50$ ps. The time dependence of the intensity at four points in the image plane B is shown in Fig. 2**a**–**d**.

In Figure 2**a** and 2**c** the pulse is lengthened; the intensity in **a** is lower than in **c** because the diffraction intensity decreases with the distance from the maximum. There is, however, no splitting of the pulse because of the simultaneous illumination of all Z-coordinates. This is not the case for the Y-coordinate, where the illuminated part changes in time. At the beginning of the propagation of the pulse along the Y-direction on the grating surface a small "Y-width" of the grating is illuminated. A broad intensity distribution results in the image plane B with a considerable intensity at a selected distance from the centre of the image. If the pulse illuminates the central part of the grating with the maximum "Y-width", then there occurs a contraction of the intensity distribution at B. The intensity at the selected point decreases. If the pulse propagates close to the second grating edge the intensity increases again. This is shown in Figs. 2**b** and 2**d**.

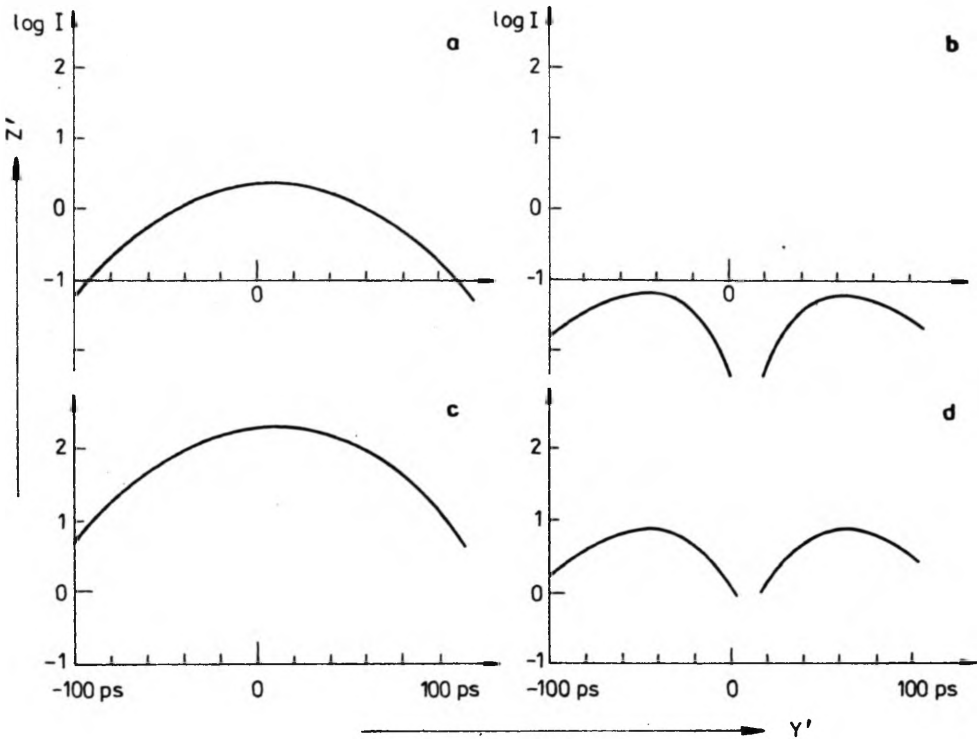

Fig. 2. Time-dependent intensity for a diffracted 50 ps-pulse at four positions in the image plane $B(Y', Z')$: **a** $-(Y', Z') = (0, A)$, **b** $-(Y', Z') = (A, A)$, **c** $-(Y', Z') = (0, 0)$, **d** $-(Y', Z') = (A, 0)$, $A = 2.5 \times 10^{-4}$ cm

The maximum intensity corresponding to Fig. 2**d** increases in comparison with Fig. 2**a** if we add, for instance, a comatic aberration. This meridional coma can be "produced" by changing the applied wavelength of the grating from the stigmatic wavelength $\lambda_0 = 458$ nm into $\lambda_0 = 468$ nm. The corresponding pulses in the image plane, with $Z = 0$ and at 6 different Y-positions, are shown in Fig. 3.

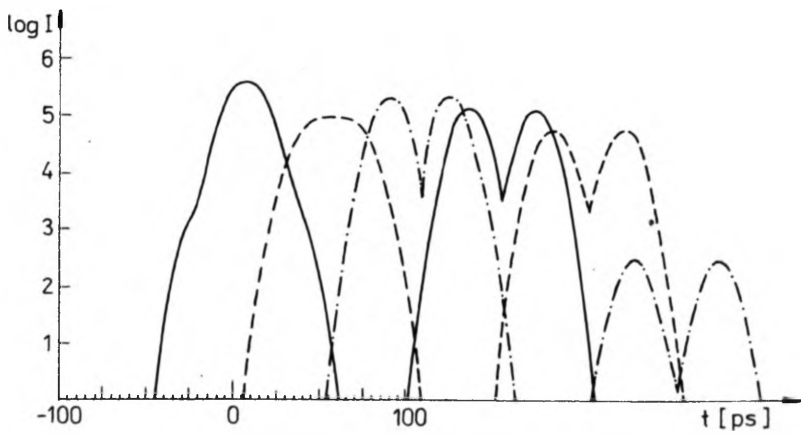

Fig. 3. Pulse shape at six different image positions, form left to right: $Y' = 0$, 2.5, 5, 7.5, 10 and 50 μm, $Z' = 0$

Now we consider an example with a triple pulse derived from a Lloyds mirror-type grating used in earth satellites of the "intercosmos programme" [8]. The manufacturing configuration is $l_C = 20.46$ cm, $\gamma = 41.753°$, $l_D = 18.\ 215$ cm, $\delta = -2.662°$ (polar coordinates of points C and D), $R = 18.34$ cm (radius of curvature of the support), $\lambda = 458$ nm. The polychromator configuration has the parameters of use $l_A = 22.267$ cm, $\alpha = 45.976°$ (polar coordinates of split A). In Figure 4**a** light pulse of 50 ps with $\lambda_0 = 822.9$ nm is shown in the central image point $Y' = Z' = 0$ (Fig. 4**a**), in the point $Y' = 25$ μm, $Z' = 0$ (Fig. 4**b**) and in the point $Y' = Z' = 0$, adding, however, $5 \times 10^{-5}\ Y^2 - 3 \times 10^{-7}\ Y^4$ to the light path function (Fig. 4**c**). The different signs for defocusing D and spherical aberration S in the last example are chosen for the demonstration of the effect.

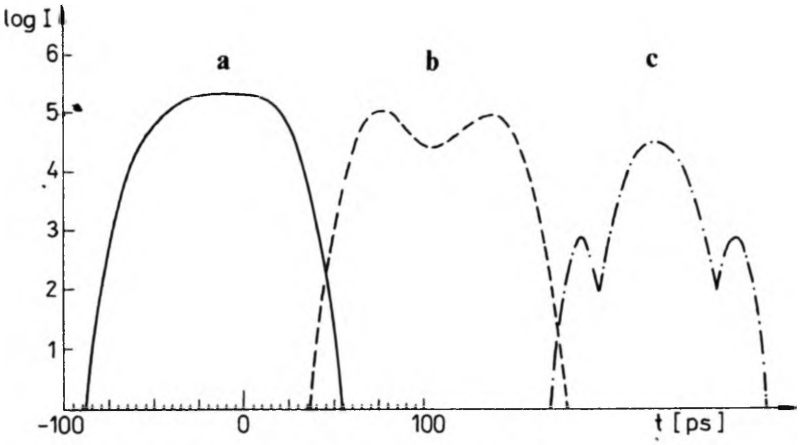

Fig. 4. Double and triple pulses by grating diffraction

The side pulses could not be increased due to the difficulties related to the diffraction integral convergence by using large aberrations. In calculation shown in Figs. 3 and 4, the Z-integration was neglected in order to simplify the problem.

5. Images by ray tracing

As the example of ray tracing calculations we took the above-mentioned grating [8]. We have assumed in the model that the receiver of radiation sumps up the whole intensity contained in a narrow slit which has an infinite extension perpendicular to the dispersion direction. All the resulting pulses are normalized to equal maximum values.

Firstly, we treat the case of defocusing with a 30 ps rectangular pulse for $\lambda_0 = 822.9$ nm. We do not focus to the spectroscopically preferred meridional focusing position, but to the sagittal focusing position. We obtain a moving focus depicted in Fig. 5. A similar intensity moving in a receiver plane is shown in [12].

Secondly, we demonstrate the turning motion at $\lambda_0 = 700$ nm (30 ps-pulse)

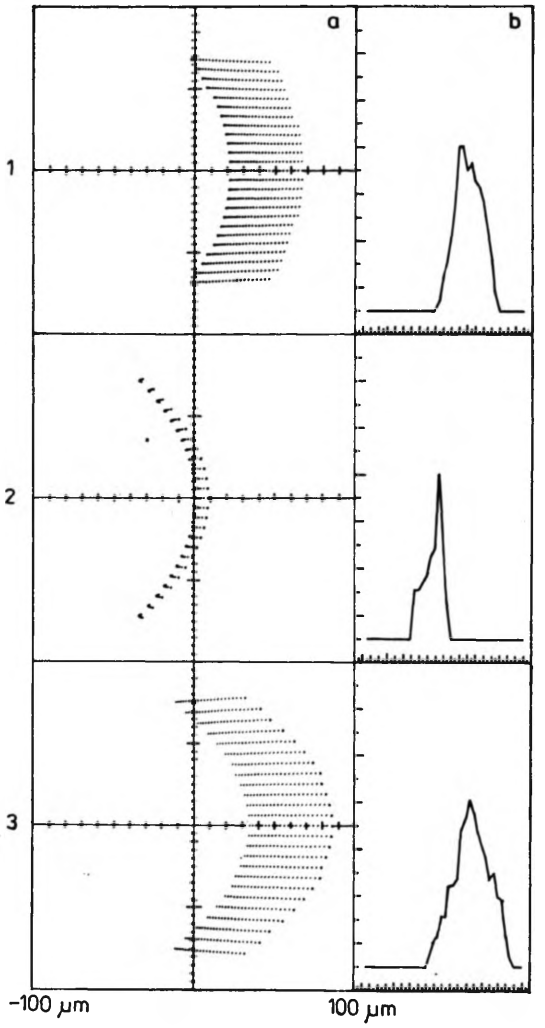

Fig. 5. Movement of the focus: **a** – spot diagrams for different times, **b** – intensities derived from ray tracings. 1 – $t = -120$ ps, 2 – $t = 0$, 3 – $t = 120$ ps

caused by meridional coma (Fig. 6). Now the focusing distance in the meridional focusing position. The curvature of the spectral line results in a spread of the intensity profile, but the turning motion of the intensity is demonstrated. The effect is marked by a shortening of the pulses if we perform integration over a limited vertical extension of the receiving slit. The pure ray tracing does not include the diffraction. But the 30 ps-pulse gives a width $w \approx 2$ cm on the grating, and this width results in a diffraction width $w' \approx 0.001$ cm, i.e., smaller than the details of the ray tracing figures.

Thirdly, we demonstrate a double turning by adding to the case of Fig. 5 ($\lambda_0 = 822.9$ nm, 15 ps-pulse) exaggerated defocusing and spherical aberration to the light path function $-4 \times 10^{-2}\, Y^2 + 4 \times 10^{-3}\, Y^4$. The results is shown in Fig. 7.

Triple pulses may occur at fixed space points. The aberrations added in the last case for producing these triple pulses are greater than those we can find for well corrected gratings. We exaggerated for demonstrating the principle.

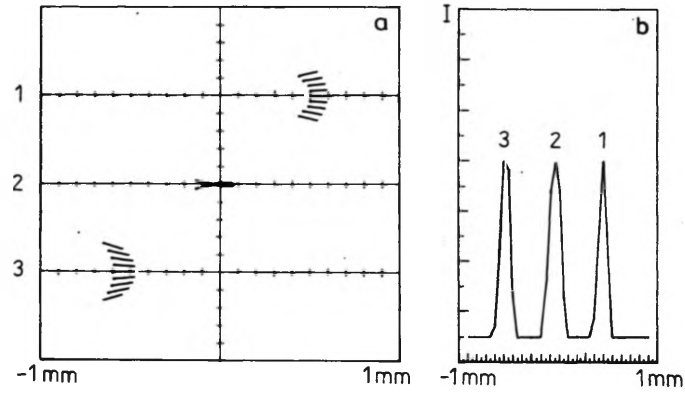

Fig. 6. Spot diagrams (**a**) and slit-integrated intensities (**b**) for meridional coma: $1-t = -30$ ps, $2-t = 40$ ps, $3-t = 100$ ps

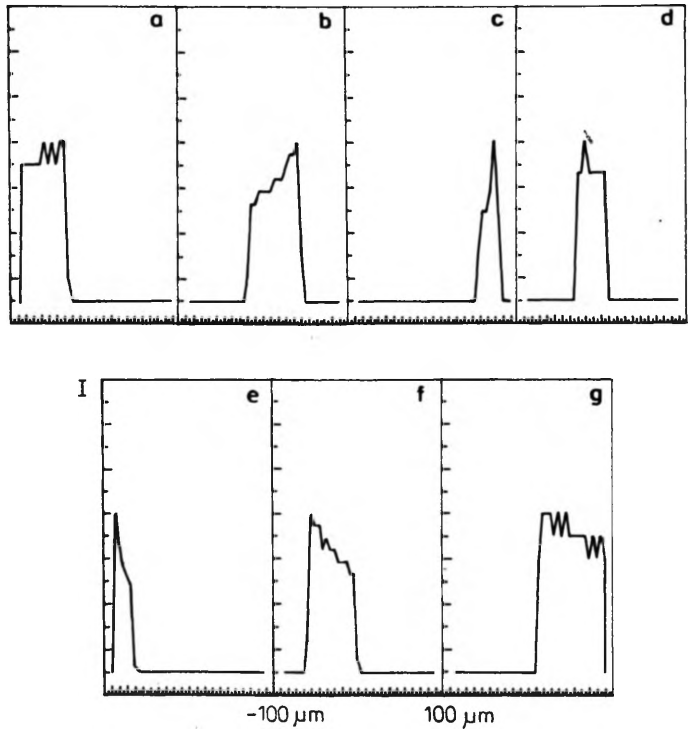

Fig. 7. Double turning of intensity: **a** $-t = -120$ ps, **b** $-t = -100$ ps, **c** $-t = -80$ ps, **d** $-t = 0$, **e** $-t = 80$ ps, **f** $-t = 100$ ps, **g** $-t = 120$ ps

6. Discussion

If the receiver has a wrong position in the image plane, then the pulse lengthened by the grating can be split into multiple pulses. The neighbouring spectral lines may disturb the pulse shape if the comatic tail reaches the centre of the receiver. In general, the astigmatic curvature of the spectral line will smooth this effect if a lengthened receiving slit is used. We have, however, shown the cases, where a lengthened slit does not suppress this effect. In usual gratings with a spectral interval of 400 ... 500 nm there are ranges where multiple pulses occur mixted with ranges where they do not exist. If multiple pulses are required, then appropriately large aberrations can be obtained by the construction of concave gratings, e.g., by the methods given in [7]. We can extend the holographic aspect: prescribed spatial movements of the focus can be obtained by synthetic holograms used for light deflection [13], where the hologram moves through the laser beam. The same effect can be obtained if the short pulse moves over the hologram (or grating) in the same manner as discussed above.

References

[1] *Jenaer Rundschau, Information 1985*, special issue, p. 19.
[2] VIENOT J. C., GOEDGEBUER J. P, FERRIERE R., CALATRONI J., SALCEDO J., *Optics in Four Dimensions–1980* [Ed.] M. A. Machado, L. M. Narduci, AIP New York 1981, pp. 49, 71, 73, 418.
[3] GASE R., SCHUBERT M., Opt. Acta **29** (1982), 1331; **30** (1983), 1125.
[4] GASE R., Opt. Quantum Electron. **16** (1984), 117.
[5] GÜTHER R., Proc. IV Intern. Symp. *Ultrafast Phenomena in Spectroscopy*, Reinhardsbrunn, GDR, October 23–26, 1985, [Eds.] P. K. Kryukov, Yu. M. Popov, p. 123.
[6] BOR Z., III Intern. Symp. *OPTIKA'88*, Budapest, Hungary, September 13–16, 1988, will be published in J. Mod. Opt. and Opt. Lett.
[7] GÜTHER R., Opt. Appl. **11** (1981), 413.
[8] GÜTHER R., POLZE S., KORN G., Optik **72** (1986), 71.
[9] BORN M., WOLF E., *Principles of Optics*, Pergamon Press, Oxford 1964, p. 378.
[10] KIRCHHOFF G., *Vorlesungen über mathematische Physik*, Vol. 2, *Mathematische Optik*, Teubner, Leipzig 1891, p. 27.
[11] HUTLEY M. C., *Diffraction Gratings*, Academic Press, London 1982, p. 243.
[12] POLLAND H. J., ELSAESSER T., SEILMEIER A., KAISER W., KUSSLER M., MARX N. J., SENS B., DREXHANGE K. H., Appl. Phys. B **32** (1983), 53.
[13] SCHREIER D., *Synthetische Holographie*, Fachbuchverlag, Leipzig 1984.

Received January 10, 1989
in revised version August 8, 1989

Влияние аберрации на отображение кратких импульсов света через вогнутую голографическую сетку

Рассмотрено влияние корригированной, голографической вогнутой дифракционной сетки на образ краткого импульса света при применении расчетов зависимого от времени хода лучей, а также зависимой от времени теории дифракции. Импульс был удлинен на время, необходимое для сканирования сетки. Этот удлиненный импульс может быть разложен на многие импульсы вследствие аберрации.